ELSEVIER

Journal of Neuroscience Methods 129 (2003) 105–113

JOURNAL OF NEUROSCIENCE METHODS

www.elsevier.com/locate/jneumeth

A template for spatial normalisation of MR images of the rat brain

Petra Schweinhardt [a,b], Peter Fransson [a], Lars Olson [b], Christian Spenger [a,b,*], Jesper L.R. Andersson [a]

[a] *Department of Clinical Neuroscience, MR Research Center, Karolinska Institutet, S-171 77 Stockholm, Sweden*
[b] *Department of Neuroscience, Retzius väg 8, Karolinska Institutet, S-171 77 Stockholm, Sweden*

Received 18 March 2003; received in revised form 9 May 2003; accepted 9 June 2003

Abstract

In this paper, we describe the preparation of a rat template intended for use together with SPM to enable spatial normalisation of individual rat brains. The template was created from T2-weighted images of the brains of five adult female Sprague–Dawley rats. A large number of anatomical landmarks were manually identified in each of these image volumes and recorded in the appurtenant image space. The same landmarks were defined in the space of the commonly used atlas by Paxinos and Watson. For each individual volume the affine transformation that best (in a least square sense) matched the two sets of points was estimated. These transforms were used to resample the individual volumes into the "Paxinos space", and a template was created from the average of these. Hence, a rat brain spatially normalised to this template will facilitate reporting results in co-ordinates directly corresponding to the Paxinos co-ordinate system. The usage of the template is exemplified with a functional magnetic resonance imaging (fMRI) study of the somatosensory cortex of the rat. The template image volumes together with the necessary modifications to the SPM software code can be downloaded from http://mr.imaging-ks.nu/expmr.htm.

Keywords: fMRI; Template; Spatial normalisation; Sprague–Dawley; Rat brain

1. Introduction

Oxygenation-sensitive, T2*-weighted MR imaging (BOLD imaging, Ogawa et al., 1990, 1992) has since its inception proven to be a powerful technique for detecting hemodynamic correlates of cerebral neuronal activity. Presently, functional magnetic resonance imaging (fMRI) based on the BOLD response has evolved into a ubiquitous technique in neuroscience for studying different aspects of human cognition. In parallel, fMRI techniques have been adopted to study neurophysiology in animals where a substantial part of this work has been aimed at investigating the characteristics and neurophysiological basis of the BOLD response [e.g. Logothetis et al., 2001 (monkey), Smith et al., 2002 (rat)]. Whereas human fMRI studies often involve spatial normalisation to a common stereotaxic space, typically the Talairach atlas (Talairach and Tournoux, 1988), animal fMRI studies commonly report results on an individual basis in a priori-defined regions of interest. Spatial normalisation of functional neuroimaging data to a standard atlas space offers several advantages. Results can be reported in an already established stereotaxic space. Furthermore, it allows for inter-individual differences in neuroanatomy and assists inter-subject averaging, thereby increasing sensitivity to low-magnitude responses and facilitating group comparisons. Thus, spatial normalisation provides a common framework to report changes in functional activation and morphology and the means to extrapolate the results to a population level. To the authors knowledge, approaches to spatially normalise animal MRI images to a corresponding histological atlas has so far only been applied for baboon and macaque brain (Black et al., 2001a,b).

We believe that the benefits and possibilities provided by spatial normalisation—that for human fMRI investigations today is an integrated and routine preprocessing step—would be useful also in a rat fMRI setting. Studies focused on the rat brain using fMRI techniques have recently grown in popularity due to the rat's

* Corresponding author. Tel.: +46-8-728-7018; fax: +46-8-323-742.
E-mail address: christian.spenger@neuro.ki.se (C. Spenger).

0165-0270/03/$ - see front matter
doi:10.1016/S0165-0270(03)00192-4

applicability as animal model for a variety of human diseases and genetic traits. Pertinent examples are rat fMRI studies of stroke (Sauter et al., 2002), Parkinson's disease (Pelled et al., 2002), pain (Malisa and Docherty, 2001), anxiety (Kalisch et al., 2002), the action of neuropharmacological drugs (Marota et al., 2000; Houston et al., 2001; Xu et al., 2000) and hypothalamic function (Mahankali et al., 2000).

In this communication we present a template of the rat brain that is aligned in space to the atlas of Paxinos (Paxinos and Watson, 1982). The Paxinos atlas was chosen since it offers detailed anatomical information and is the histological rat brain atlas most widely used in neuroscience. The template is based on MR images of five adult female Sprague–Dawley rats. As severe susceptibility artefacts render the preparation of a template of the whole rat brain based on T2*-weighted images less reliable we based our MRI template on T2-weighted images. It is implemented within the SPM99 software package (Wellcome Department of Cognitive Neurology, London, UK; http://www.fil.ion.ucl.ac.uk/spm). The functionality of the rat image template is exemplified in fMRI experiments where the left or right forepaw was electrically stimulated in a blocked paradigm. The maximum of activation in the rat somatosensory cortex is given in space co-ordinates relating to the Paxinos atlas.

2. Materials and methods

2.1. Subjects

The rat brain template was constructed from high-resolution T2-weighted images acquired in five female Sprague–Dawley rats (B&K Universal, Sollentuna, Sweden). Functional MRI was performed in two of these rats. One additional rat underwent anatomical and functional MR imaging for an assessment of the reliability and validity of the template. The weight of the animals ranged from 200 to 250 g. All experiments were approved by the Stockholm animal ethics committee.

2.2. Animal preparation and electrical stimulation

Anesthesia was induced with 1–1.5% isoflurane/halothane. One (template experiments) or two (fMRI experiments) catheters were inserted in the tail vein(s). Animals were orally intubated and artificially ventilated ($f = 75$ per min, $N_2{:}O_2 = 2{:}1$). Complete muscle relaxation was achieved by administration of pancuronium bromide (0.5 mg/kg body weight per h i.v., Organon, Oss, Netherlands). The rats were placed in the scanner using a MR compatible fixation device securing the animals head with a tooth bar. Body temperature was maintained at 36–37 °C using warm air. For fMRI experiments, anaesthesia was switched to α-chloralose. After administration of a bolus (60 mg α-chloralose/kg body weight i.v., Sigma, Stockholm, Sweden), halothane was discontinued. Throughout the experiment, α-chloralose was continuously infused at a rate of 20 mg/kg body weight per h. For electrical stimulation, bipolar electrodes were implanted subcutanously in the right and left forepaw, respectively. Stimulation was performed using a 1 mA current pulse (500 μs pulse length, frequency 3 Hz). The activation protocol consisted of eight or ten repetitive cycles with 10 s of stimulation and 40 s of rest.

2.3. MR image acquisition

Magnetic resonance imaging was performed on a 4.7 T spectrometer with a 40 cm horizontal bore (Bruker Biospec Avance 47/40, Bruker, Karlsruhe, Germany). A volume coil (Bruker) with an inner diameter of 35 mm was used for MR signal transmission and detection. Initially, both T1- and T2-weighted high resolution images were acquired to determine the MR image tissue contrast that was best suited to delineate neuroanatomical landmarks in the rat brain. T1-weightening was achieved by using an Inversion Recovery sequence (TR/TI/TE = 3000/400/19 ms) whereas T2-weightening was accomplished using a RARE (Hennig et al., 1986) imaging sequence using a repetition time (TR) of 5800 ms and an effective echo time (TE) of 52.5 ms. Direct comparisons revealed that anatomical landmarks were to an equal degree visible in the T1-weighted images and T2-weighted images, respectively. Due to the substantial reduction in scanning time compared with T1-weighted image acquisition, we chose to base the rat brain template on T2-weighted image volumes. Whole brain coverage was accomplished in five rats by coronal (following histological convention) T2-weighted images with a spatial resolution of $0.117 \times 0.117 \times 0.5$ mm^3 (FOV = 30×30 mm^2, 256×256 matrix size, 0.5 mm slice thickness). In one rat, a smaller FOV of 25×25 mm^2 was used yielding a voxel size of $0.098 \times 0.098 \times 0.5$ mm^3. Except for one rat, a RARE-factor of 8 was used and 16 image acquisitions were averaged together (acquisition time = 54 min) to increase the signal-to-noise ratio. In the remaining rat, a RARE-factor of 32 was used and 32 image acquisitions averaged (acquisition time = 27 min). Detection of BOLD responses in the rat brain with focus on somatosensory cortex was accomplished by acquiring either five or ten coronal images centred 5 mm posterior to the rhinal fissure using a spiral trajectory gradient echo sequence. T2*-sensitivity was achieved by using a flip angle of $\alpha = 22.5°$ and an echo time of 40 ms (TR = 325 ms). Other MR image acquisition parameters were an interrepetition delay of 35 ms, a matrix size equal to 64×64, FOV = 40×40

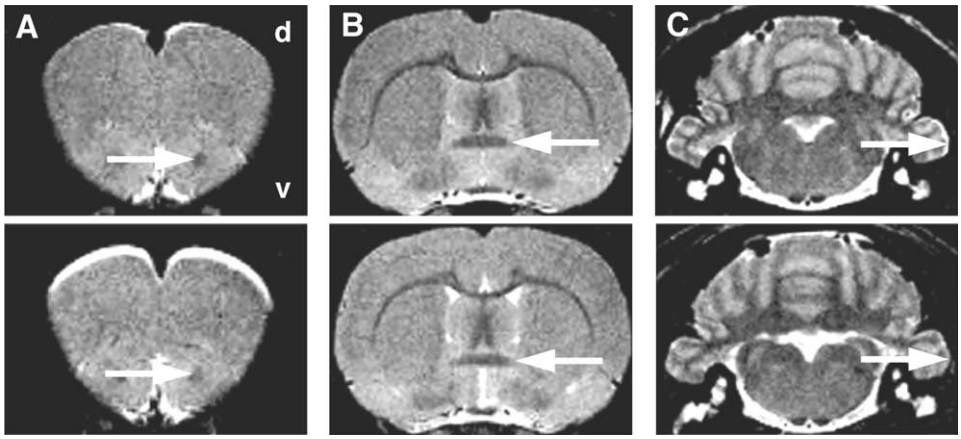

Fig. 1. Three coronal sections from two different rat brains (upper and lower row) demonstrating three selected anatomical landmarks used in the construction of the MRI template. White arrows point in (A) at the center of the anterior part of the anterior commisure, in (B) at the lateral boundary of the posterior part of the anterior commisure, and in (C) at the lateral-most point of the paraflocculus. d, dorsal; v, ventral.

mm^2, slice thickness = 1 mm, no slice gap, interleaved acquisition (three interleaves) and an acquisition time of 1010 ms per repetition. In total, 540 (five slices) or 440 (ten slices) repetitions were performed resulting in an experimental time between 7 and 9 min.

2.4. Alignment of the MR images to the Paxinos atlas

We based the alignment of the T2-weighted image space and the Paxinos atlas space upon a label-based affine spatial transformation. Homologous anatomical features in the two image spaces were identified and used to find the affine transformation that best superimposed the labelled points. To obtain accurate estimates of the transformation parameters, we aimed at identifying as many reliable anatomical structures as possible (Evans et al., 1989). In addition, we sought for an even spatial spread of the selected points across the rat brain volume. Forty-nine anatomical landmarks were identified on the high-resolution T2-weighted images in one arbitrarily chosen rat and determined in the remaining four rats. This is exemplified in Fig. 1 that shows the anatomical location for three of the determined landmarks in two different rats. However, the set of anatomical landmarks are not all to an equal degree visible and reliably identified in the T2-weighted images. We, therefore, subjectively rated each labelled point. The rating of a landmark was based on its visibility and clearness across all animals. Four of the landmarks were rated as extremely well defined (rating: ++++), 15 as very well defined (+++), 24 as well defined (++), and six as satisfactory (+) defined. A full account of all anatomical landmarks and their individual ratings are given in Table 1.

The affine transform that minimised the weighted least square distance between the Paxinos co-ordinates and the spatial co-ordinates obtained from each individual T2-weighted image volume was calculated. This was done for all five T2-weighted image volumes. A diagonal covariance matrix with the elements consisting of the reciprocal of the ratings was used. The resulting degree of correspondence between the two point sets is demonstrated in Fig. 2 for one rat in a sagittal, coronal and horizontal view. A comparison of the spatial distributions of the transformed point lists revealed only very small differences in the brains of five different rats. In four rats, no outliers were detected at all, whereas in one rat, the landmark "caudate putamen" (CPu) was bilaterally an outlier and, therefore, not included in the further analysis. In the same rat, the landmark "anterior commisure, intrabulbar part" (aci, bilaterally) showed as well a slight mismatch with the corresponding Paxinos co-ordinates. However, we decided to retain these points in the list since they were the only ones that resided in the frontal part of the rat brain. The finding of a very small inter-individual variance for the point lists was the basis of our decision not to include more than five individuals in the construction of the template.

2.5. Design of the MR image template

After realignment, each individual T2-weighted image volume was resampled into a volume that encompassed the spatial extent of the Paxinos atlas. To this end, we used a bounding box of −8 to +8 mm in the x-direction (left–right), −12 to +1 mm in the y-direction (ventral–dorsal) and −15.6 to +6 mm in the z-direction (posterior–anterior). The voxel size was set to $0.2 \times 0.2 \times 0.2$ mm, resulting in a volume of $80 \times 63 \times 108$ voxels. The individual, resampled, images were histogram-equalised and averaged to create a "mean" rat brain in the Paxinos space (in the following referred to as canonical image volume).

The Paxinos atlas provides two separate zero-reference planes, where one is related to the interaureal line

Table 1
List of anatomical landmarks defined on the MR images

Structure	Abbreviation	Localisation of measurement	Side	Lat	D–V	A–P	Rating
Anterior commisure, posterior part	acp	Lateral-most point	r	1.26	7.03	−0.3	++++
			l	−1.26	7.03	−0.3	++++
Fornix	f	Midline		0	5.95	−0.3	++++
Posterior commisure	pc	Midline		0	5.15	−4.8	++++
Anterior commisure, intrabulbar part	aci	Dorsal-most point	r	1.9	5.29	5.2	+++
			l	−1.79	5.34	5.2	+++
Anterior commisure, anterior part	aca	Center	r	1.87	6.71	3.2	+++
			l	−1.87	6.71	3.2	+++
Mamillothalamic tract	mt	Center	r	0.95	7.67	−2.8	+++
			l	−0.95	7.67	−2.8	+++
Lateral habenular nucleus	LHb	Lateral-most point	r	1.03	4.81	−3.3	+++
			l	−1.03	4.81	−3.3	+++
Aqueduct (Sylvius)	Aq	Center		0	5.44	−6.3	+++
Pyramidal tract	py	Dorsal-most point	r	0.58	10.5	−10.3	+++
			l	−0.58	10.5	−10.3	+++
Paraflocculus one	PF1	Lateral-most point	r	7.27	7.6	−11.3	+++
			l	−7.27	7.6	−11.3	+++
Paraflocculus two	PF1	Lateral-most point	r	6.77	7.87	−11.8	+++
			l	−6.82	7.98	−11.8	+++
Forceps minor corpus callosum	fmi	Dorsal-most point	r	1.93	3.14	2.7	++
			l	−1.93	3.2	2.7	++
Stria medullaris of thalamus	sm	Center	r	0.84	6.03	−0.8	++
			l	−0.84	6.03	−0.8	++
Optic tract	opt	Dorsal-most point	r	2.11	9.04	−1.8	++
			l	−2.01	9.04	−1.8	++
Caudate putamen (striatum)	CPu	Dorsal-most point	r	5.18	4.76	−3.8	++
			l	−5.23	4.76	−3.8	++
Mamillotegmental tract	mtg	Center	r	0.66	7.93	−4.3	++
			l	−0.66	7.93	−4.3	++
Superior thalamic radiation	str	Dorsal-most point	r	3.06	4.89	−4.3	++
			l	−2.96	4.97	−4.3	++
Central grey	CG	Lateral-most point	r	0.89	5.45	−5.8	++
			l	−0.89	5.55	−5.8	++
Motor root trigeminal nerve	m5	Medial-most point	r	2.3	9.31	−6.8	++
			l	−2.11	9.04	−6.8	++
Cerebellar lobule 3	3	Dorsal-most point		0	4.57	−9.3	++
Superior cerebellar peduncle	scp	Dorsal medial border	r	1.32	6.6	−9.3	++
			l	−1.26	6.44	−9.3	++
Dorsal tegmental nucleus	DTg	Center	r	0.31	7.24	−9.3	++
			l	−0.31	7.24	−9.3	++
Nucleus solitary tract	Sol	Center	r	1.37	8.08	−12.3	++
			l	−1.37	8.08	−12.3	++
Hypoglossal nucleus	12	Middle left and right nucleus		0	8.4	−13.3	++
			r	0.92	8.09	−3.8	+
Mamillothalamic tract	mt	Center	l	−0.92	8.09	−3.8	+
Presubiculum	PrS	Medial extension	r	4	7.3	−6.3	+
			l	n.a.	n.a.	n.a.	
Dorsal raphe nucleus	DR	Midline		0	6.08	−6.8	+
Medial geniculate nucleus	MG	Center	r	3.49	6.13	−6.8	+
			l	n.a.	n.a.	n.a.	

Given are the co-ordinates in the Paxinos atlas. The only exception is that for points left to the mid-line (Lat-direction) the corresponding negative values are given. The abbreviations in the second column are adopted from the Paxinos atlas. "Localisation of measurement" describes in which part of the structure the co-ordinate was determined. The landmark "Paraflocculus one" marks the most lateral extension of the whole paraflocculus whereas "Paraflocculus two" relates to the most lateral extension of this structure on slices where it is not connected to the rest of the brain. r: right side in atlas, l: left side, Lat: lateral, D–V: dorsal–ventral, A–P: anterior–posterior, n.a.: not assessed because not shown in Paxinos atlas.

and the other to bregma. For the MRI adaptation of Paxinos space, we selected the bregma reference plane. The spatial co-ordinate system given in the Paxinos atlas does not differentiate between left and right hemisphere (Lat-direction). To avoid any ambiguities, we arbitrarily defined the x-axis in the MR template to be negative to the left of the mid-line and to be positive to the right. Furthermore, we decided to swap the y- and z-axes in

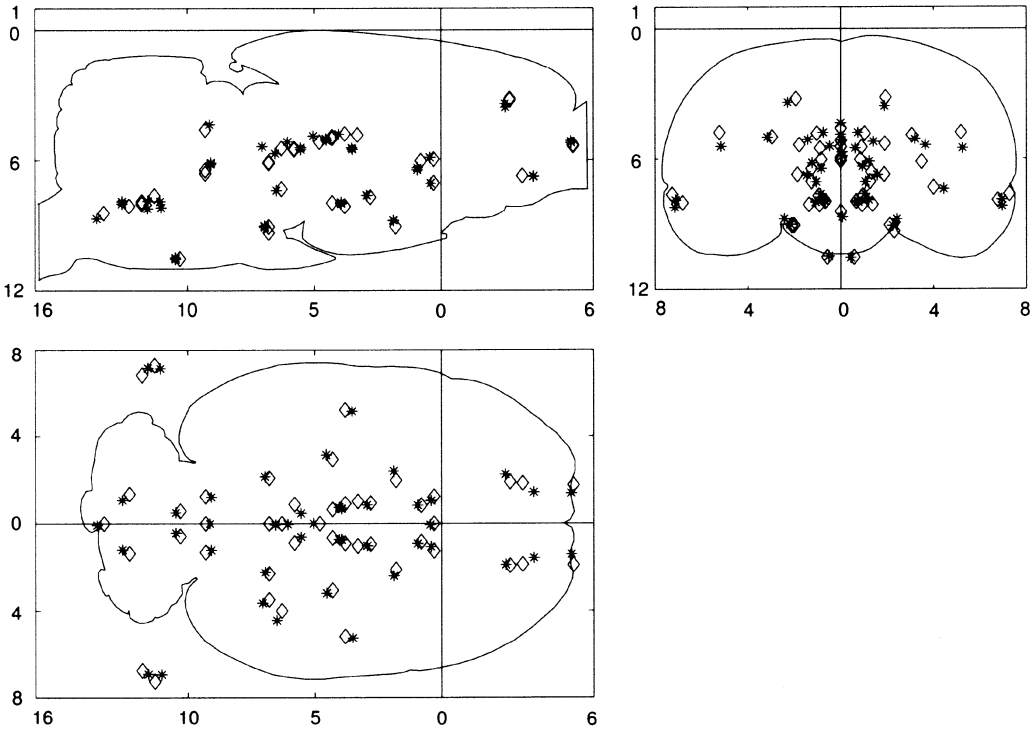

Fig. 2. An example of spatial correspondence achieved between the anatomical landmarks defined in a T2-weighted image and the corresponding co-ordinates in the Paxinos atlas. Points marked with '*' signify the MR space, whereas points denoted '◇' belong to the Paxinos atlas space. Top left—sagittal; Top right—coronal and Bottom left—coronal view.

SPM such that the "new" y-axis and z-axis are aligned to the posterior–anterior and the ventral–dorsal direction, respectively. This was done for pragmatic reasons since the resulting layout used the space available for display more efficiently. Also, we used units of a tenth of a millimetre rather than millimetre since this choice enabled a one-to-one relationship between the co-ordinates of the Paxinos atlas and the voxels within the maximum intensity projection (MIP) display in SPM. For the interpretation of a given co-ordinate within SPM, it is important to note that the axes in the Paxinos atlas are denoted Lat/A–P/D–V instead of x, y and z. Taken together, this implies that a co-ordinate reported as [8 −14 −62] in SPM is to be interpreted as the position [0.8 −1.4 −6.2] in Paxinos space, i.e. 0.8 mm right of the mid-line, 1.4 mm posterior to bregma and 6.2 mm ventral to the horizontal plane that intersects bregma (anteromedial thalamic nucleus). Finally, the mean MR rat brain template was spatially smoothed using a filter with a full width half maximum (FWHM) of 0.8 mm^3. This can equivalently be seen as a lowpass filtering of the images and thereby decreasing sharp contrast gradients in the images. A reduction of high contrast gradients in the template facilitates the finding of a least-square solution between the two image volumes (Friston et al., 1995a,b). In addition, a binary version (mask image) of the rat image template was created.

2.6. Co-registration of functional and anatomical MR images

The presence of large susceptibility artefacts in the T2*-weighted images, in particular in the cerebellum and olfactory bulb, severely hampered a direct use of automated co-registration procedures that are based on computing similarity measures between the T2*- and T2-weighted image volumes. In this situation an alternative, albeit less sophisticated approach is to use the information of the geometrical relationship between the two image volumes (slice orientation, FoV, offset in x-, y- and z-direction) given by the MRI scanner. This strategy was employed in this study where the two image volumes had identical spatial orientation and extent in both the x- and y-direction with the only difference being a small offset in the z-direction. Hence, the functional image volume was co-registered to the anatomical volume by a translation (in the z-direction) of the T2* image volumes using the information about the slice offset factor given in the image file header.

2.7. Data analysis of the functional MR images

The functional data sets were all preprocessed and statistically analysed within the SPM99 software package. First, the T2-weighted image volumes were used to find

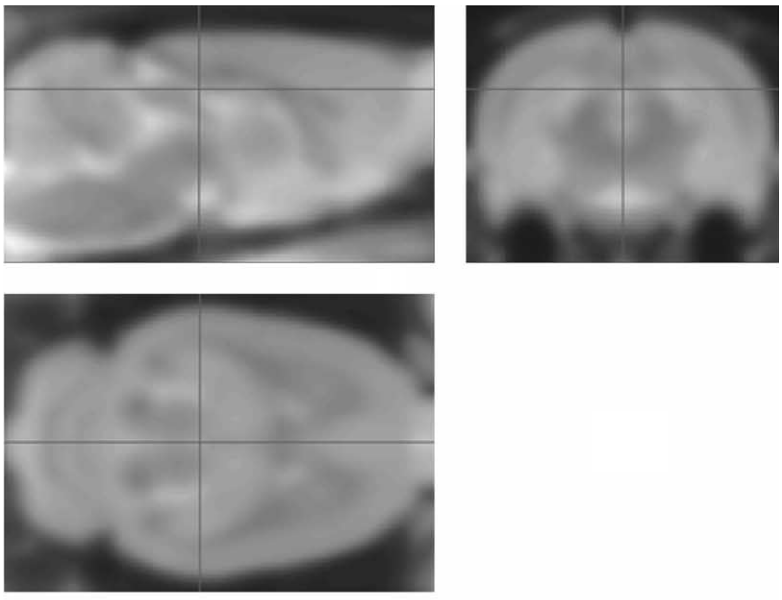

(A)

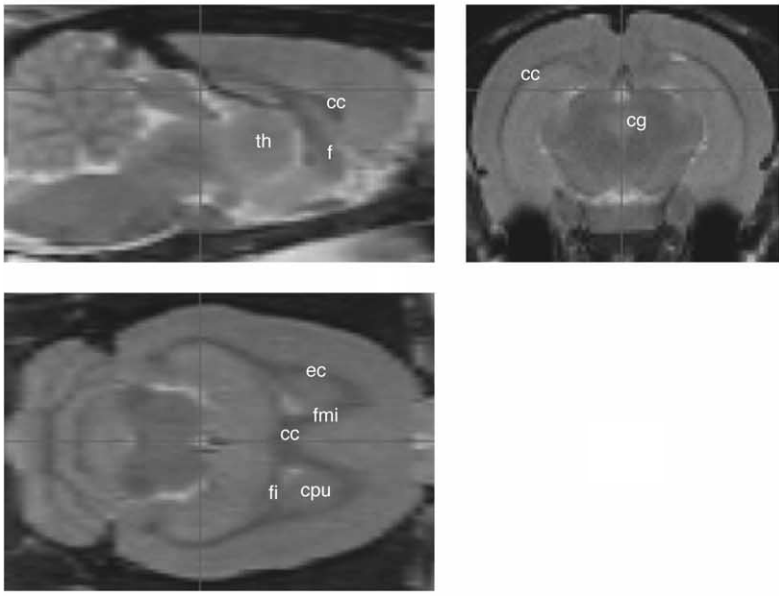

(B)

Fig. 3. MRI template of the rat brain. (A) Sagittal, coronal and horizontal views (the intersection point of the three orthogonal planes corresponds to X = 0.0, Y = −5.7, Z = −3.6 in Paxinos space) of the spatially smoothed version of the MRI template. (B) A canonical, unfiltered version of the MRI template to be used for overlay purposes. cc, corpus callosum; f, fornix; th, thalamus; cg, central grey; ec, external capsule; fi, fimbria hippocampus; fmi, forceps minor; cpu, caudate putamen.

the transform to the MR image template. The functional images were resampled using the same transform and thereafter spatially filtered using an isotropic Gaussian kernel with a FWHM of three voxels. In addition, temporal filtering was applied using a high pass filter of 0.01 Hz and a Gaussian low pass filter with FWHM = 4 s. Proportional scaling was applied to account for global confounds. The canonical hemodynamic response function in SPM was used to model the main effect of interest, that is electrical stimulation versus rest. Finally, voxel-based statistical tests for activated brain regions were performed in individual rats at $P \leq 0.05$, corrected for multiple comparisons.

3. Results and discussion

The overall shape and quality of the MRI template is presented in a finalised form in Fig. 3. The top panel (Fig. 3A) shows in three orthogonal projections the

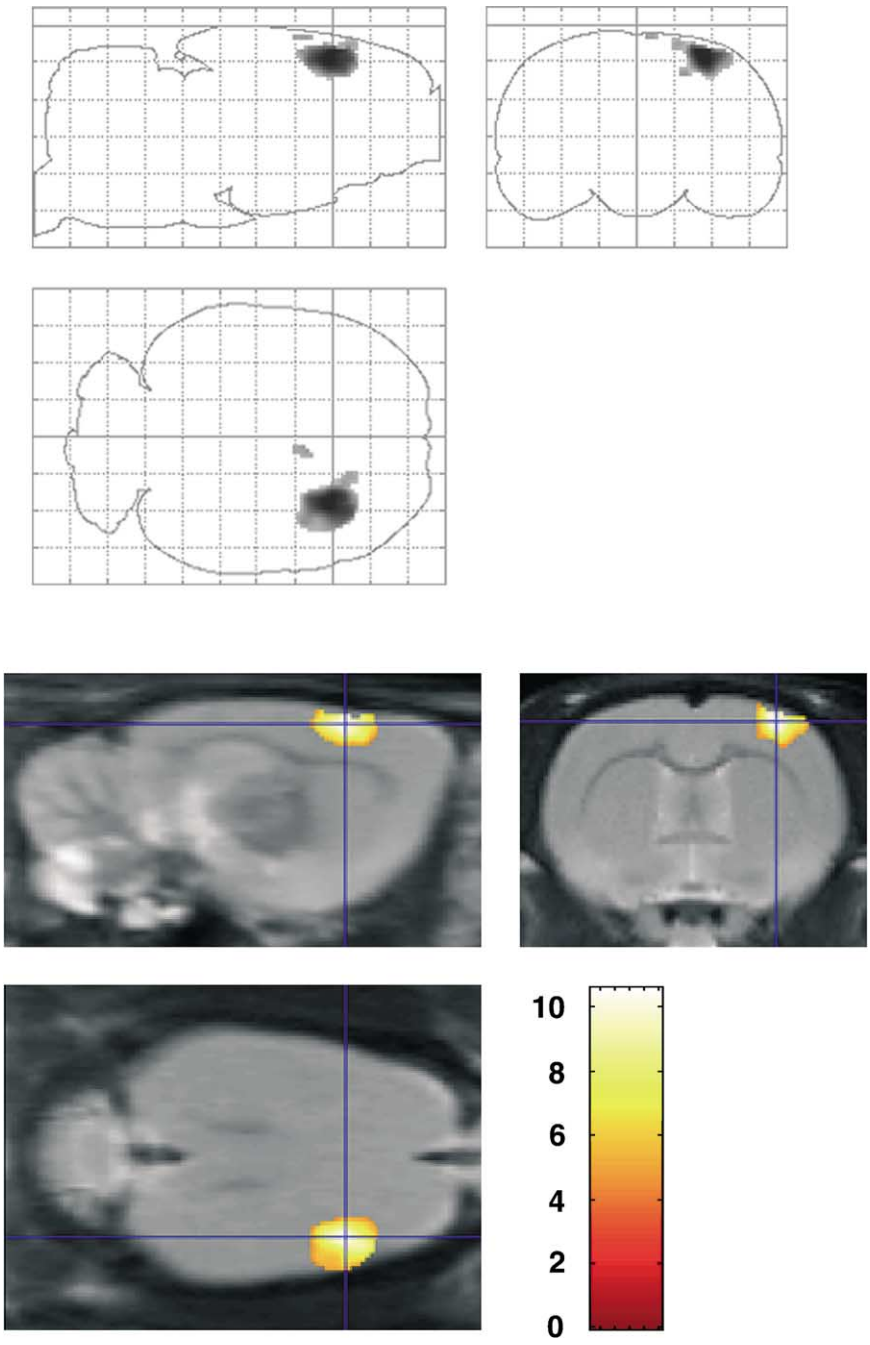

Fig. 4. Activation of the right somatosensory cortex following electric stimulation of the left forepaw in an individual rat. The top panel shows in a MIP (“glass brain view”) activation of the contralateral somatosensory cortex. The bottom panel shows activated brain regions as color-coded areas superimposed onto the canonical template. The peak of activation was located at X = −3.6, Y = −1.8, Z = −0.2 in Paxinos space (T = 10.55, $P \leq 0.05$, corrected for multiple comparisons).

spatially smoothed version meant to serve as a template for spatial normalization of MR images to the space defined by the Paxinos atlas. The bottom panel (Fig. 3B) shows the canonical, unfiltered version to be used for superimposition of activated brain regions onto T2-weighted MR images. Structures that can easily be seen include corpus callosum, fornix, thalamus, central grey, external capsule, fimbria hippocampus, forceps minor, and CPu.

The results from the fMRI experiments are exemplified in Fig. 4 showing the activation following electrical stimulation of the left forepaw in a single rat. In detail, the upper panel of Fig. 4 indicates a large cluster of activation in the region of the contralateral somatosensory cortex given in the graphical context of a MIP representation of the rat brain. Specifically, the MIP display includes the outer contours of the rat brain (as defined in selected planes of the Paxinos atlas) in a

sagittal, coronal and horizontal view, much in the same way that activations are presented in human studies within the SPM software package. Hence, the "glass brain" display provides an intuitive and easily accessible presentation of the overall spatial distribution in Paxinos space for all brain regions activated by the paradigm. The location of the maximum of activation in the cortex is shown in the lower panel of Fig. 4. Here, activated brain regions have been colour-coded and superimposed onto the canonical T2-weighted template in three orthogonal planes. The intersection point of the three planes has been set to the position of the maximum of activation (i.e. $X = -3.6$, $Y = -1.8$, $Z = -0.2$) which is attributed to the right somatosensory cortex according to the Paxinos atlas. This finding is in good agreement with previous fMRI investigations of the rat somatosensory cortex (e.g. Spenger et al., 2000). The functional data shown stem from the one rat that was not used in the preparation of the template. Similar patterns of activation in the right (left, respectively) somatosensory cortex were obtained in two rats used for the template in which additionally stimulation of the left (right, respectively) forepaw was performed (data not shown).

In summary, we have described the construction of an MRI template that together with the SPM software package allows for spatial normalisation of individual rat brains to the Paxinos standard space. The usage and applicability of the template was demonstrated with an example where BOLD correlates of neuronal activity in the rat brain could be identified and assigned to the somatosensory cortex as defined in the Paxinos atlas. It should be noted that the template is based on the brains of female Sprague–Dawley rats, which renders it most suitable for spatial normalisation of such animals. When there is a cause to believe that large differences in neuroanatomy exist, such as differences in gender or strain, the template is to be used with caution. However, for brains which are larger as a whole the template is suitable as such scaling difference is taken care of by the scaling parameters in the affine model that are used in the spatial normalization step. Therefore, the template can be used without restrictions for female Sprague–Dawley rats with a higher body weight.

The rat brain MRI template together with the necessary modifications of the SPM software package are freely available on the internet and can be downloaded from http://mr.imaging-ks.nu/expmr.htm.

Acknowledgements

Supported by the Swedish Research Council, AMF, Hedlunds Stiftelse and United States Public Health Services. P.F. was supported by a grant from the Swedish Brain Foundation. The spiral sequence was implemented on our Bruker system by S. Månsson, Department of Experimental Research, University Hospital of Malmö, Malmö, Sweden and T. Klason, Experimental MR Unit, Department of Clinical Neuroscience, Karolinska Institutet, 17176 Stockholm, Sweden. We are indebted to the authors of SPM for making public the software package that the implementation of the rat brain MRI template is based upon.

References

Black KJ, Snyder AZ, Koller JM, Gado MH, Perlmutter JS. Template images for non-human primate neuroimaging: 1. Baboon. NeuroImage 2001a;14:736–43.

Black KJ, Koller JM, Snyder AZ, Perlmutter JS. Template images for non-human primate neuroimaging: 2. Macaque. NeuroImage 2001b;14:744–8.

Evans AC, Marret S, Collins L, Peters TM. Anatomical–functional correlative analysis of the human brain using three-dimensional imaging systems. SPIE Med Imag III: Image Process 1989;1092:264–74.

Friston KJ, Ashburner J, Poline JB, Frith CD, Heather JD, Frackowiak RSJ. Spatial registration and normalization of images. Hum Brain Mapping 1995a;2:165–89.

Friston KJ, Holmes AP, Worsley KJ, Poline JP, Frith CD, Frackowiak RSJ. Statistical parametric maps in functional imaging: a general linear approach. Hum Brain Mapping 1995b;2:189–210.

Hennig J, Nauerth A, Friedburg H. RARE imaging: a fast imaging method for clinical MR. Magn Reson Med 1986;3:823–33.

Houston GC, Papadakis NG, Carpenter TA, Hall LD, Mukherjee B, James MF, Huang CL. Mapping of brain activation in response to pharmacological agents using fMRI in the rat. Magn Reson Imag 2001;19:905–19.

Kalisch R, Wigged A, Gössl C, Czisch M, Landgraf R, Auer DP. BOLD-phMRI response to diazepam depends on innate emotionality in rats—differential involvement of prefrontal cortex, Proceedings of International Society of Magnetic Resonance in Medicine, 10th Scientific Meeting, Honolulu, 2002. p. 1357.

Logothetis NK, Pauls J, Augath M, Trinath T, Oeltermann A. Neurophysiological investigation of the basis of the fMRI signal. Nature 2001;412:150–7.

Mahankali S, Liu Y, Pu Y, Wang J, Chen C-W, Fox P, Gao J-H. In vivo fMRI demonstration of hypothalamic function following intraperitoneal glucose administration in a rat model. Magn Reson Med 2000;43:155–9.

Malisa KL, Docherty JC. Capsaicin as a source for painful stimulation in functional MRI. J Magn Reson Imag 2001;14:341–7.

Marota JJ, Manderville JB, Weisskoff RM, Moskowitz MA, Rosen BR, Kosofsky BE. Cocaine activation discriminates dopaminergic projections by temporal response: an fMRI study in rat. NeuroImage 2000;11:13–23.

Ogawa S, Lee TM, Key AR, Tank DW. Brain magnetic resonance imaging with contrast dependent on blood oxygenation. Proc Natl Acad Sci USA 1990;87:9868–72.

Ogawa S, Tank DW, Menon R, Ellermann JM, Kim SG, Merkle H, Ugurbil K. Intrinsic signal changes accompanying sensory stimulation: functional brain mapping with magnetic resonance imaging. Proc Natl Acad Sci USA 1992;89:5951–5.

Paxinos G, Watson C. The Rat Brain in Stereotaxic Coordinates, second ed. Sydney: Academic Press, 1982.

Pelled G, Bergman H, Goelman G. Bilateral overactivation of the sensorimotor cortex in the unilateral rodent model of Parkinson's

disease—a functional magnetic resonance study. Eur J Neurosci 2000;15:389–94.
Sauter A, Reese T, Porszasz R, Baumann D, Rausch M, Rudin M. Recovery of function in cytoprotected cerebral cortex in rat stroke model assessed by functional MRI. Magn Reson Med 2002;47:759–65.
Smith AJ, Blumenfeld H, Behar KL, Rothman DL, Shulman RG, Hyder F. Cerebral energetics and spiking frequency: the neurophysiological basis of fMRI. Proc Natl Acad Sci USA 2002;99:10765–70.
Spenger C, Josephson A, Klason T, Hoehn M, Schwindt W, Ingvar M, Olson L. Functional MRI at 4.7 tesla of the rat brain during electric stimulation of forepaw, hindpaw, or tail in single- and multislice experiments. Exp Neurol 2000;166:246–53.
Talairach J, Tournoux P. Co-Planar Stereotaxic Atlas of the Human Brain. Stuttgart: Thieme Medical, 1988.
Xu H, Li SJ, Bodurka J, Zhao X, Xi ZX, Stein EA. Heroin-induced neuronal activation in rat brain assessed by functional MRI. Neuroreport 2000;11:1085–92.